Chinese Journal of Physiology 61(2): 92-105, 2018
DOI: 10.4077/CJP.2018.BAG561

High-Frequency Stimulation of the Subthalamic Nucleus Activates Motor Cortex Pyramidal Tract Neurons by a Process Involving Local Glutamate, GABA and Dopamine Receptors in Hemi-Parkinsonian Rats

Chi-Fen Chuang[1, #], Chen-Wei Wu[2, #], Ying Weng[2], Pei-San Hu[1], Shin-Rung Yeh[1], and Yen-Chung Chang[2]

[1]Institute of Molecular Medicine, National Tsing Hua University, Hsinchu 30013
and
[2]Institute of Systems Neuroscience, National Tsing Hua University, Hsinchu 30013, Taiwan, Republic of China

Abstract

Deep brain stimulation (DBS) is widely used to treat advanced Parkinson's disease (PD). Here, we investigated how DBS applied on the subthalamic nucleus (STN) influenced the neural activity in the motor cortex. Rats, which had the midbrain dopaminergic neurons partially depleted unilaterally, called the hemi-Parkinsonian rats, were used as a study model. c-Fos expression in the neurons was used as an indicator of neural activity. Application of high-frequency stimulation (HFS) upon the STN was used to mimic the DBS treatment. The motor cortices in the two hemispheres of hemi-Parkinsonian rats were found to contain unequal densities of c-Fos-positive (Fos^+) cells, and STN-HFS rectified this bilateral imbalance. In addition, STN-HFS led to the intense c-Fos expression in a group of motor cortical neurons which exhibited biochemical and anatomical characteristics resembling those of the pyramidal tract (PT) neurons sending efferent projections to the STN. The number of PT neurons expressing high levels of c-Fos was significantly reduced by local application of the antagonists of non-N-methyl-D-aspartate (non-NMDA) glutamate receptors, gamma-aminobutyric acid A ($GABA_A$) receptors and dopamine receptors in the upper layers of the motor cortex. The results indicate that the coincident activations of synapses and dopamine receptors in the motor cortex during STN-HFS trigger the intense expression of c-Fos of the PT neurons. The implications of the results on the cellular mechanism underlying the therapeutic effects of STN-DBS on the movement disorders of PD are also discussed.

Key Words: deep brain stimulation, dopamine receptors, motor cortex, Parkinson's disease, subthalamic nucleus

Corresponding authors: [1] Dr. Yen-Chung Chang, Institute of Systems Neuroscience, National Tsing Hua University, 101 Kung-Fu Rd. Sec. 2, Hsichu 30013, Taiwan, ROC. Tel: +886-3-5742754, Fax: +886-3-5715934, E-mail: ycchang@life.nthu.edu.tw; [2] Dr. Shin-Rung Yeh, Institute of Molecular Medicine, National Tsing Hua University, 101 Kung-Fu Rd. Sec. 2, Hsinchu 30013, Taiwan, ROC, Tel: +886-3-574-2690, Fax: +886-3-5715934, E-mail: sryeh@life.nthu.edu.tw.
[#]Authors contributed equally to this work.
Received: September 20, 2017; Revised: December 10, 2017; Accepted: January 12, 2018.
 ISSN : 0304-4920. http://www.cps.org.tw

Introduction

Parkinson's disease (PD) is globally the second most common debilitating neurodegenerative disorder, only after Alzheimer's disease. The pathological hallmark of PD is the gross degeneration of dopaminergic neurons in the substantia nigra pars compacta (SNpc). The motor symptoms of PD include tremor at rest, bradykinesia, akinesia, muscular rigidity and unstable posture. In addition to various medications (35, 37, 57), deep brain stimulation (DBS) is also used widely to treat PD patients whose symptoms cannot be controlled satisfactorily by medications alone (30).

DBS involves the delivery of high-frequency electrical stimuli to deep-lying nuclei, such as the subthalamic nucleus (STN) and internal globus pallidus of the brains of PD patients *via* long electrodes implanted in the brain (2, 4, 6, 16, 56, 59, 63). DBS is also used to treat other neurological and psychiatric conditions (29). Presently, our understanding of the mechanisms underlying the therapeutic effects of DBS is incomplete (11, 29, 54). Modifications aiming to improve the clinical efficacy and to minimize the potential adverse side effects of the current DBS technology have presently been investigated (8, 13, 44, 61, 65).

The motor cortices of PD patients and PD model animals exhibit neurochemical, anatomical and functional abnormalities (46). By means of optogenetics and electrophysiology, it has been demonstrated that STN-DBS induces antidromic activities which propagate from the STN region to the motor cortex, thereby influencing the activity of layer V neurons in the motor cortex and producing therapeutic effects (24, 42). Stimulating the motor cortex of PD patients by transcranial magnetic stimulation, or by electric shocks, also produces anti-parkinsonian effects (18, 25). These results suggest that the motor cortex plays important roles in the therapeutic effects of STN-DBS on alleviating the movement symptoms of PD.

Here, by using c-Fos expression as an indicator (9, 14), we studied how high-frequency stimulation (HFS) applied on the STN affected the neural activity of the motor cortex in hemi-Parkinsonian rats, which are a widely used animal model of PD (45, 48). We found that STN-HFS rectified the bilateral imbalance of the neuronal activity in the motor cortices in the two hemispheres. In particular, the pyramidal tract (PT) neurons sending projections to the STN (38, 58) were found to be intensely activated by a process involving the non-N-methyl-D-aspartate (non-NMDA) glutamate receptors, gamma-aminobutyric acid A ($GABA_A$) receptors and dopamine receptors residing in the upper layers of the motor cortex. The implications of our results to the cellular mechanisms underlying the therapeutic effects of STN-DBS on the motor symptoms of PD are discussed.

Materials and Methods

Hemi-Parkinsonian Rats

Male Sprague-Dawley rats (9-10 week-old, weight ~280 g) were purchased from Bio-LASCO Taiwan Co., Ltd. (Taipei, Taiwan). All experimental procedures involving rats used in this study adhered to the animal guidelines of the National Tsing Hua University Institutional Animal Care and Use Committee (approval document No. 10321). Hemi-Parkinsonian rats were produced by applying 6-hydroxydopamine (6-OHDA) onto the medial forebrain bundle according to the procedures reported by Perese *et al*. (60). Two weeks after the 6-OHDA injection, rats were subjected to amphetamine (Taiwan Food and Drug Administration)-induced rotation test (28), and rats rotated >6 turns/min were used in subsequent experiments, and were referred to as "hemi-Parkinsonian rats". Rats receiving injection of phosphate-buffered saline (PBS) (6 μl) by the same procedure were referred to as "control rats". A total of 65 rats were used in this study, including 49 hemi-Parkinsonian and 16 control rats.

Electrophysiology

Stimulation electrodes were made from two Teflon-insulated tungsten wires (inner diameter, I.D., 50.8 μm; outer diameter, O.D., 101.6 μm; #795500, A-M Systems, Carlsberg, WA, USA) placed individually in stainless steel cannulas (30G1/2", Becton, Dickinson and Company, NJ, USA) with the wire tips separated by a distance of ~400 μm. Two to three weeks after receiving PBS or 6-OHDA injection, a stainless reference steel wire (127 μm in diameter, #791500, A-M Systems) was inserted in the contralateral cerebellum to a depth of 8 mm. This reference electrode was used when the ends of the stimulation electrodes were positioned in the STN in the lesioned side (anterior–posterior, AP −3.8 mm, medial–lateral, ML +2.75/L +3.25 mm, dorsal–ventral, DV −7.6 mm). During this latter implantation process, the stimulation electrodes were used to detect the signature activities of the STN. Finally, the stimulation and reference electrodes were fixed to the skull by using dental acrylic (Hygenic repair resin, Hygenic, Akron, OH, USA) and ten stainless steel anchor screws. Biphasic symmetrical pulses at 130 Hz, pulse width of 60 μs and current of 100 μA, or as otherwise indicated, were delivered into

STN *via* the stimulation electrodes by using an isolated pulse stimulator (Model 2100, A-M Systems).

Recording electrodes were made from stainless steel wires (50 μm in diameter; #304 HFV, California Fine Wire, Grover Beach, CA, USA) shielded by polyimide tubing individually (I.D., 127 μm; O.D., 165 μm; #823200, A-M Systems). The tip of the recording electrode was positioned in layer Vb of the motor cortex (AP +2.5, ML +2.5, DV -2.5 mm). A bare platinum wire (127 μm in diameter, #773000, A-M Systems) implanted in the brain (AP +2.5, ML 0 mm) at a depth of ~6 mm was used as the reference electrode. Four weeks after electrode implantation, local field potentials (LFPs) were recorded from freely moving rats *via* the recording electrode. Signals recorded were sequentially amplified 20 times by an 8 channel-headstage preamplifer (Triangle Biosystems, Inc., Durham, NC, USA) and then 100 times and bandpass-filtered (0.1-5 k Hz) by an amplifier (Differential alternating current, AC amplifier model 1700, A-M Systems), digitalized into 8-bit signals at 20000/sec sampling rate (AD/DA convertor, NI-6221, National Instructions, Austin, TX, USA), and saved on a computer for off-line analyses. For power spectral density analyses, raw LFPs were down-sampled to 1 K and analyzed by using MATLAB script of Fast Fourier Transform (FFT).

Drug Application

For local drug applications, 1 μl of 50 μM bicuculine methochloride #0131, Tocris, St. Louis, MO, USA; a $GABA_A$ receptor antagonist), 50 μM CNQX (6-cyano-7-nitroquinoxaline-2,3-dione, #0190, Tocris; an antagonist of non-NMDA glutamate receptors), or 10 μM R(+)-SCH-23390 hydrochloride #D054, Sigma-Aldrich; a D1 dopamine receptor antagonist) plus haloperidol #H1512, Sigma-Aldrich; a D2 dopamine receptor antagonist) in PBS or PBS alone was delivered into layers II/III or layer V of the motor cortex by using an injection module. An injection module consisted of a guidance cannula (23G Terumo® Needle, #140718, Terumo Co.) and was fixed on the skull above the dura 2 weeks prior to experiments. Right before the drug injection experiments, an injection cannula (30G Terumo® Dental Needle, #150413, Terumo Co.) was inserted through the guidance cannula and extended 2 and 4 mm from the ventral end of the guidance cannula to reach layers II/III and layer V of the motor cortex (respectively at: AP +2.5, ML +2.5, DV -1 mm and AP +2.5, ML +2.5, DV -2.5 mm), respectively. Drug solution and PBS were administered at a flow rate of 0.5 μl/min. The injection cannula was removed 5 min after completing the injection.

Fast Blue Retrograde Labeling

Fast Blue (2.5 μg in 1 μl PBS, #17740; Polysciences Inc., Eppelheim, Germany) was injected into the STN (AP −3.8 mm, ML +3.0 mm, DV −7.6 mm) *via* a 30 G injection cannula placed in the brain by inserting through a 23 G stainless steel guidance cannula placed between the bipolar stimulation electrodes above the dura. Fast Blue was injected at a flow rate of 0.5 μl/min, and the injection cannula was retracted 5 min after finishing the injection.

Detecting c-Fos Expression by Immunohistochemical Staining with 3,3'-Diaminobenzidine (DAB)

Rat brains were fixed by the intracardiac perfusion procedures as described earlier by Gage *et al*. (19). Coronal sections of 40 μm in thickness were prepared by using a freezing sliding microtome (Leica CM305S, Leica Microsystems, Wetzlar, Germany) and then kept in PBS containing 0.1% (w/v) sodium azide at 4°C. For examining c-Fos expression, sections were sequentially incubated in PBS containing 0.3% (v/v) Triton X-100 (PBST), washed three times with PBS, incubated in 0.3% (v/v) H_2O_2 in methanol for 10 min, and incubated with rabbit polyclonal antibody to c-Fos (1:500, Santa Cruz Biotechnology Cat# sc-52, RRID:AB_2106783) in PBST containing 10% (v/v) fetal bovine serum (FBS) at 4°C overnight. After washing 3 times with PBS, sections were incubated with biotinylated anti-rabbit IgG antibody (1:200, Vector Laboratories Cat# BA-1000, RRID:AB_2313606) in PBST containing 10% FBS for 30 min and then with avidin/biotinylated horseradish peroxidase complex reagents (1:100, VECTASTAIN®ABC kit, Vector Laboratories Inc., Burlingame, CA, USA) for 30 min. After washing with PBS, sections were incubated with PBS containing 0.05% (w/v) DAB and 0.015% (v/v) H_2O_2 for 15 min, washed three times with double-distilled water, and mounted onto glass slides by using ReadiUse™ microscope mounting solution (AAT Bioquest, Sunnyvale, CA, USA). Images of sections were acquired by using a microscope (Axioskop2 mot plus, Carl Zeiss MicroImaging, Inc., Thornwood, NY, USA) and a digital camera (CoolPix 4500, Nikon, Tokyo, Japan). The above procedures were also used to examine tyrosine hydroxylase (TH) expression in sections by using mouse monoclonal antibody to TH (1:200, Millipore Cat# MAB318, RRID:AB2201528) and biotinylated anti-mouse IgG antibody (1:200, Vector Laboratories Cat# BA-9200, RRID:AB_2336171).

Immunofluorescence Staining

The coronal sections containing motor cortex regions were immunofluorescence stained using a combination of rabbit polyclonal antibody to c-Fos (1:500, Santa Cruz Biotechnology Cat# sc-52, RRID: AB_2106783) and Cy3-conjugated goat anti-rabbit IgG (H+L) antibody (1:200, Jackson ImmunoResearch Labs Cat# 111-165-144, RRID:AB_2338006), or a combination of mouse monoclonal antibody to TH (1:50, Millipore Cat# MAB318, RRID: AB_2201528) and Alexa Fluor® 488-AffiniPure goat anti-mouse IgG (H+L) antibody (1:200, Jackson ImmunoResearch Labs Cat# 115-545-003, RRID: AB_2338840) by the procedures of Hsu *et al*. (33). Some sections were also double immunostained with mouse monoclonal anti-NeuN antibody (1:500, Millipore Cat# MAB377, RRID:AB_2298772), anti-GAD67 antibody (glutamic acid decarboxylase, 1:200, Millipore Cat# MAB5406, RRID:AB_2278725), or anti-non-phosphorylated neurofilament H (SMI-32) antibody (1:1000, Millipore Cat# NE1023-100UL, RRID:AB_2043449) in combination with Alexa Fluor® 488-AffiniPure goat anti-mouse IgG (H+L) antibody (1:200, Jackson ImmunoResearch Labs Cat# 115-545-003, RRID:AB_2338840). Finally, these sections were treated with 4',6-diamidino-2-phenylindole (DAPI, 10 μg/ml in PBS) at room temperature for 15 min to label the nuclei. Sections were placed under glass coverslips in ProLong Gold antifade reagent (#773938, Invitrogen/Molecular Probes, Eugene, OR, USA) and stored at 4°C. Images of sections were acquired by a microscope (Axio Observer Z1, Carl Zeiss, Jena, Germany or LSM 510, Carl Zeiss MicroImaging, Inc.).

Image and Statistical Analyses

Mosaic images of the entire motor cortex (including the M1 and M2 regions) were assembled from individual images by Adobe Photoshop software (Adobe Systems, San Jose, CA), transformed to gray scale images (between 0 and 255), and analyzed by using image J (http://rsb.info.nih.gov/ij/). Particles with gray scales <85, sizes between 20 and 300 μm^2, and circularity in the range of 0.6-1 were designated as c-Fos-positive (Fos^+)-particles, and those $c\text{-}Fos^+$-particles with gray scales <65 and sizes >100 μm^2 were designated as giant FOS^+-particles. All data were analyzed by using one-way analysis of variance (one-way ANOVA) with *post-hoc* Tukey Honestly Significant Difference.

Results

Characterization of the Hemi-Parkinsonian Rats

Immunohistochemical staining of the brain sections prepared from the hemi-Parkinsonian rats by using an antibody to TH revealed the depletions of TH-positive dopaminergic neurons in the SNpc and ventral tegmental area (VTA) and diminished dopaminergic processes in the striatum in the lesioned side (Fig. 1A, right panels). In sections prepared from the control rats, the TH-immunostaining patterns in the two sides were not distinguishable (Fig. 1A, left panels). Four weeks after 6-OHDA injection, exaggerated oscillations in the β-regime (between 25 and 40 Hz) were detected in the layer Vb of the motor cortex of the hemi-Parkinsonian rats (Fig. 1B, right top panel), but not in the same brain region of the control rats (Fig. 1B, left top panels). The power of β-oscillations in the hemi-Parkinsonian rats was attenuated by applying a HFS (130 Hz) onto the STN in the lesioned side, and β-oscillation power was attenuated more when HFS of higher currents was applied (Fig. 1B and Fig. 1C, middle and bottom right panels). Upon STN-HFS, the overall mobility of the hemi-Parkinsonian rats increased noticeably. Application of STN-HFS during the amphetamine-induced rotation tests could stop and sometimes reverse the direction of the rotation movement of the animals. The positions of stimulation electrodes in the STN were verified at the end of the experiments (Fig. 1D). The described characteristics were consistent with those of hemi-Parkinsonian rats as described in earlier reports (5, 15, 24, 34, 36).

c-Fos Expression in the Motor Cortex

We examined the c-Fos expression in the motor cortices of four groups of rats, including control rats without being or had been subjected to STN-HFS, and hemi-Parkinsonian rats without being or had been subjected to STN-HFS for 4 h, which were referred to as CTL, CTL-S, PD and PD-S rats, respectively (Fig. 2A). Immunuohistochemical staining of the brain sections prepared from these animals using an anti-c-Fos antibody resulted in the detection of numerous $c\text{-}Fos^+$-particles over the entire motor cortex region (Fig. 2B). However, due to large variations among individual animals, we did not detect differences bearing statistical significances between any two of these samples with respect to the density of $c\text{-}Fos^+$-particles in different layers of the motor cortex region (Fig. 2D). To minimize differences among individual animals, the motor cortex in the intact side of each animal was used as the internal control of its motor cortex in the lesioned side and the ratios of the $c\text{-}Fos^+$-particle density in the motor cortices in the injection side (the lesioned side in PD and PD-S rats and the sham-injection side in CTL and CTL-S rats) to those in the intact side of the above animals

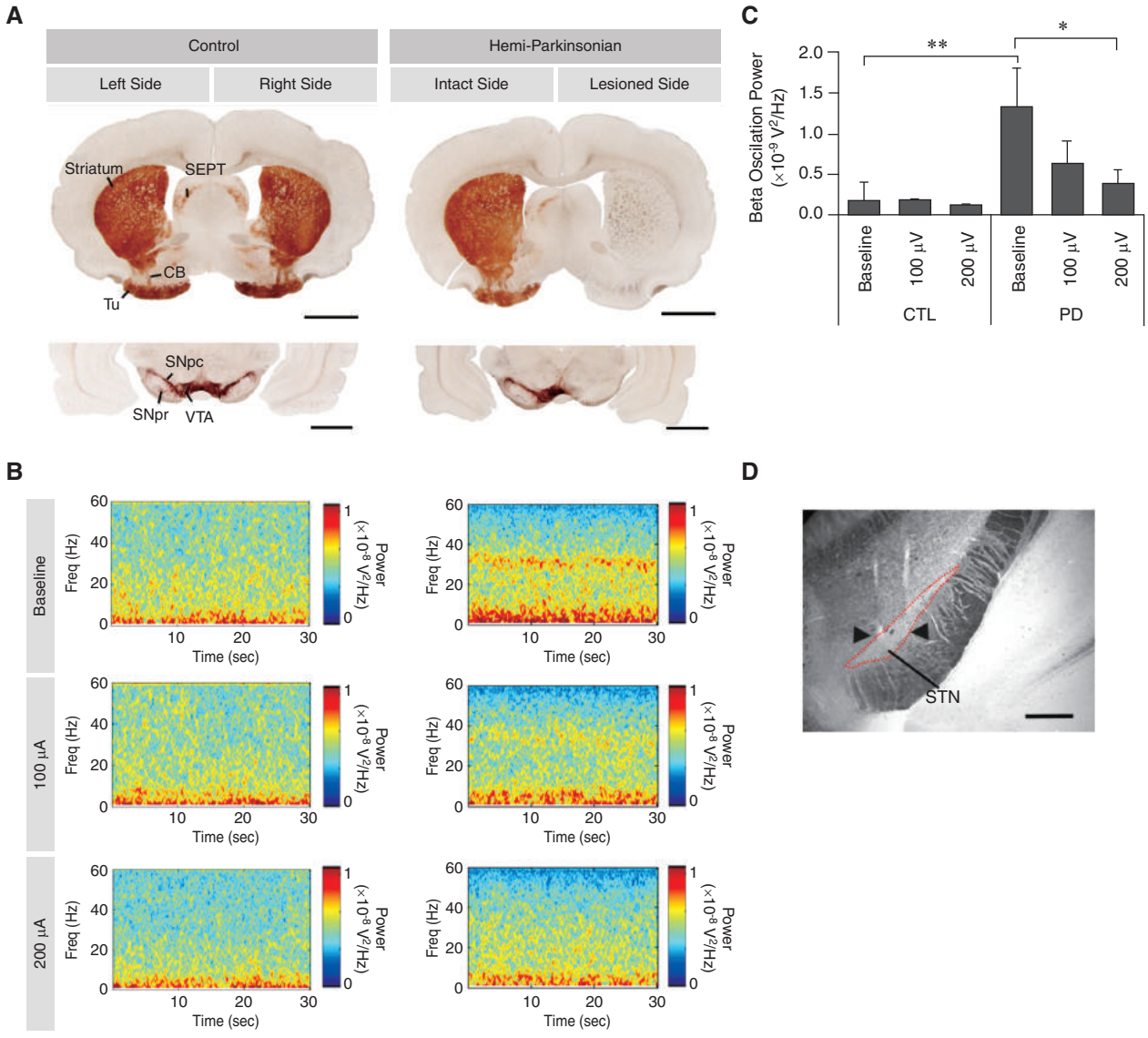

Fig. 1. Characterization of hemi-Parkinsonian rats. (A) TH expression in the coronal sections prepared from a control rat (left) and a hemi-Parkinsonian rat (right) containing striatum (top images) and substantia nigra (SN, bottom images). Abbreviations: Tu, olfactory tubercle; SEPT, septum; CB, cell bridges ventral striatum; SNpc, SN pars compacta; SNpr, SN pars reticulate; VTA, ventral tegmental area. Scale bars: 2 mm. (B) Time-frequency power spectra of LFPs respectively recorded from layer Vb of M1 of a control rat (left panel) and a hemi-Parkinsonian rat (right panel) 4 weeks after 6-OHDA injection and before (Baseline, top panel) and during the application of STN-HFS at current intensities of 100 μA (middle panel) and 200 μA (bottom panel). (C) Quantification of the powers of β-oscillations in the motor cortices of control and hemi-Parkinsonian rats before and during the application of STN-HFS at current intensities of 100 and 200 μA. Data are mean ± standard deviation (S.D.) from 3 animals. *$P < 0.05$ and **$P < 0.01$. (D) Verification of the location of the bipolar stimulating electrodes (arrowheads) within the STN. Scale bar: 500 μm.

were calculated. The resultant ratios were called the c-Fos$^+$-particle ratios (Fig. 2E). The c-Fos$^+$-particle ratios of the control rats were found to be close to 1 and not affected by STN-HFS. In the hemi-Parkinsonian rats, on the other hand, the c-Fos$^+$-particle ratios were lower than those of the control rats. However, STN-HFS raised the c-Fos$^+$-particle ratios of the hemi-Parkinsonian rats to a level comparable to those of the control rats, *i.e.* a ratio of ~1. Furthermore, in the internal segment of Globus Pallidus (GPi), the number of c-Fos$^+$-particles of PD rats was higher than in the control rats, with the particle densities in GPi, 23.6 ± 5.9 per mm^2 (n = 3) in PD rats *vs*. 7.7 ± 3.5 per mm^2 (n = 3) in control rats ($P < 0.01$, one-way ANOVA). After STN-HFS, the number of c-Fos$^+$-particles in the GPi of PD rats decreased (23.6 ± 5.9

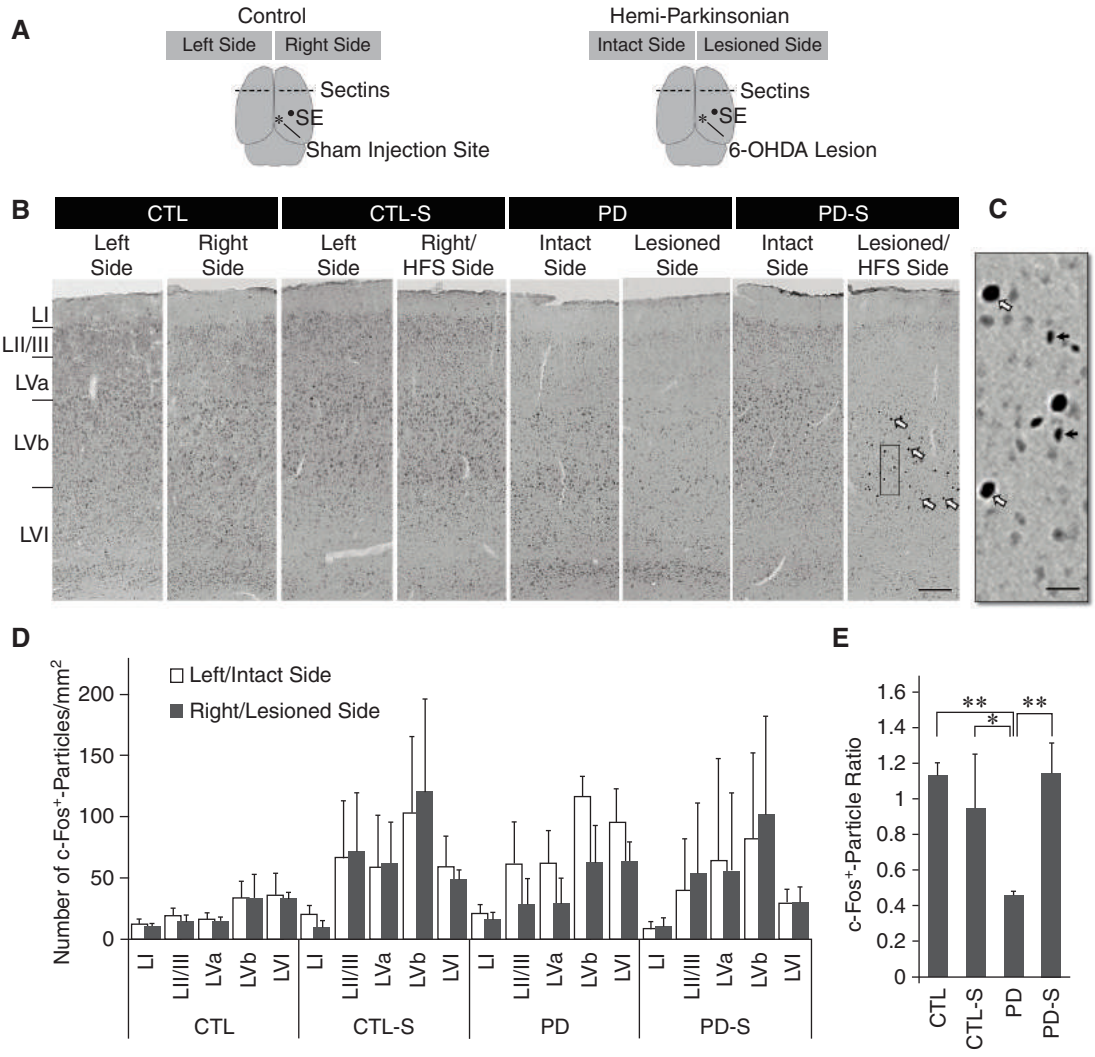

Fig. 2. Analysis of c-Fos expression in the motor cortices of control and hemi-Parkinsonian rats before and after STN-HFS. (A) Sites of operations in the brain of control (left) and hemi-Parkinsonian (right) rats. SE indicates the site of stimulation electrodes. (B) c-Fos expression in the motor cortex contralateral and ipsilateral to the injection site (the 6-OHDA-injection or lesioned side in PD and PD-S rats and sham-injection side in CTL and CTL-S rats) of control and hemi-Parkinsonian rats with and without subjecting to STN-HFS for 4 h, respectively labeled as CTL, CTL-S, PD and PD-S. Four giant FOS^+-particles are indicated by arrows as examples. Scale bar: 200 μm. (C) The image of the area enclosed by the black rectangle in the right panel of PD-S in Fig. 2B at a higher magnification. Two giant FOS^+-particles are indicated by open arrows and two of the remaining c-Fos^+-particles are indicated by black arrows as example. Scale bar: 30 μm. (D) Quantification of the density of c-Fos^+-particles, *i.e.* the number of c-Fos^+-particles per mm^2, in different layers of the motor cortex in the intact (open bars) and lesioned (closed bars) side of the rats. (E) The ratios of c-Fos^+-particle density in the motor cortex in the injection (or lesioned) side to that in the intact side as calculated from the rats. Data shown in (C) and (D) are the means ± S.D. from 3 animals. $*P < 0.05$ and $**P < 0.01$.

per mm^2 (n = 3) in the PD rats *vs*. 2.5 ± 2.9 per mm^2 (n = 3) in the PD-S rats ($P < 0.01$). This observation is in accordance with the notion that the GPi/substantia nigra pars reticulata (SNr) becomes hyperactive in PD and that the GPi/SNr hyperactivity is inhibited by HFS-DBS (11). Interestingly, many large c-Fos^+-particles with strong staining intensities were consistently noted in the motor cortices in the lesioned side of the PD-S rats; examples are indicated by open arrows in the right panel under PD-S in Fig. 2B and in Fig. 2C. However, only a few of such large and dark particles were found in the motor cortices in the intact side of the same animals (Fig, 2B, left panel under PD-S). Such large and dark c-Fos^+-particles were also seldom found in the motor cortices of CTL or CTL-S or in the motor cortices of the PD rats (Fig. 2B, panels under CTL, CTL-S and PD). Quantitative analyses also revealed a population of large and

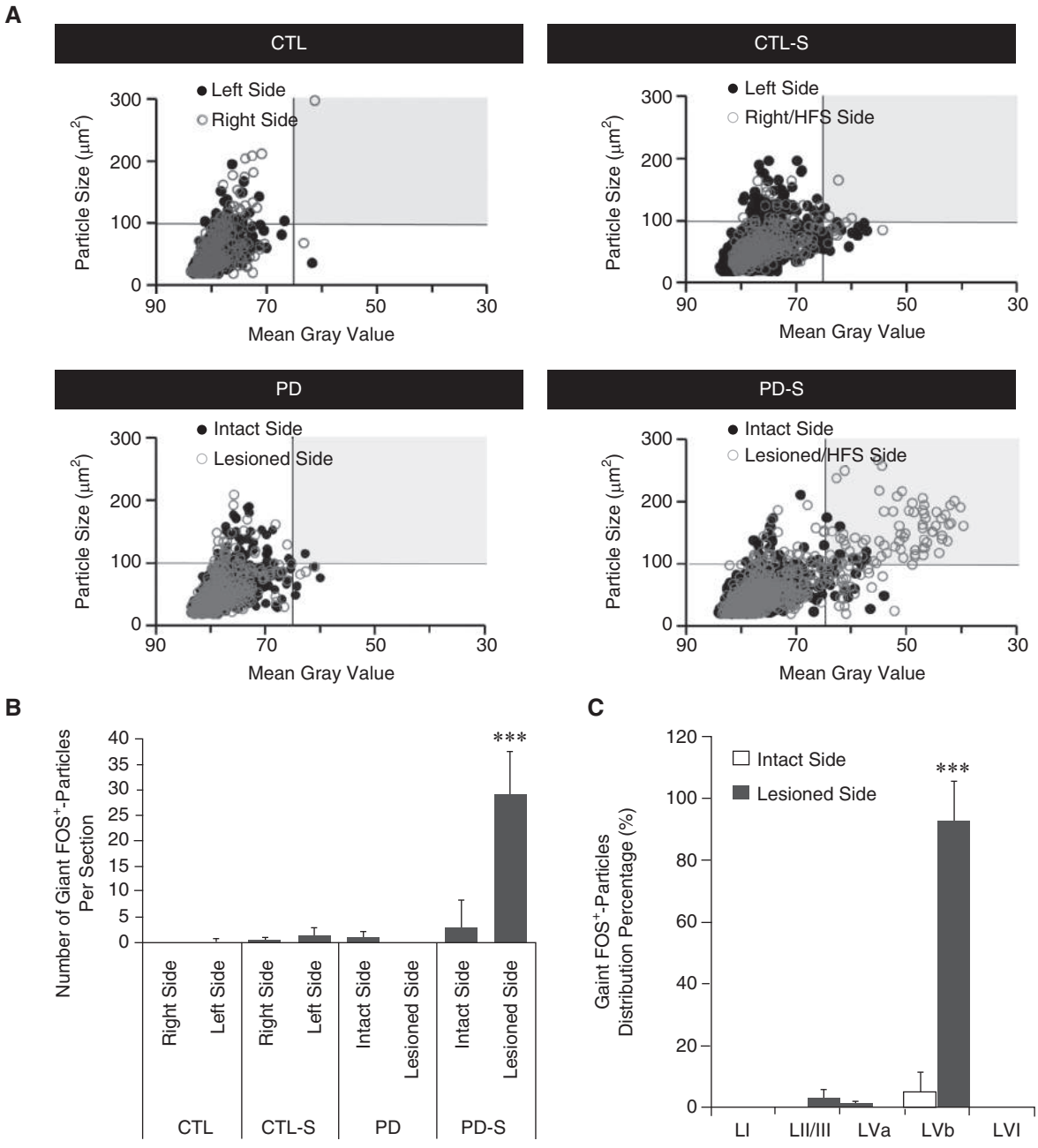

Fig. 3. Quantitative analyses of the size and relative darkness of the c-Fos$^+$-particles (A) Scatter plots of the size (area, μm^2) versus the staining darkness (mean gray values) of c-Fos$^+$-particles in the motor cortices of CTL, CTL-S, PD and PD-S rats. For each condition, data from 6 slices prepared from 3 animals are included in analysis. (B) Numbers of the giant FOS$^+$-particles (size >100 μm^2, and mean gray value <65) in the motor cortex of each section prepared from the rats. (C) Distributions of giant FOS$^+$-particles in LI, LII/III, LVa, LVb and LVI of motor cortices in the lesioned (dark bars) and intact (open bars) sides of PD-S rats. Data shown in (B) and (C) are the means ± S.D. from 3 animals. ***$P < 0.001$ versus all other groups or layers.

dark particles with sizes >100 μm^2 and mean gray values <65, as those found in the top right quadrants in the panels of Fig. 3A; these particles were designated as giant FOS$^+$-particles. In the motor cortex region in the lesioned side of each section pre pared from the PD-S rat, 29.0 ± 8.5 (mean ± S.D., n = 3) giant FOS$^+$-particles were found. On the other hand, few giant FOS$^+$-particles were found in the motor cortical region of each of the sections prepared from the intact side of PD-S or in those prepared from either side of the CTL and CTL-S rats (Fig. 3B). It was further found that the majority of giant FOS$^+$-particles found in the motor cortex, 92.2 ± 6.7% (n = 3), resided in layer Vb of this brain region (Fig. 3C).

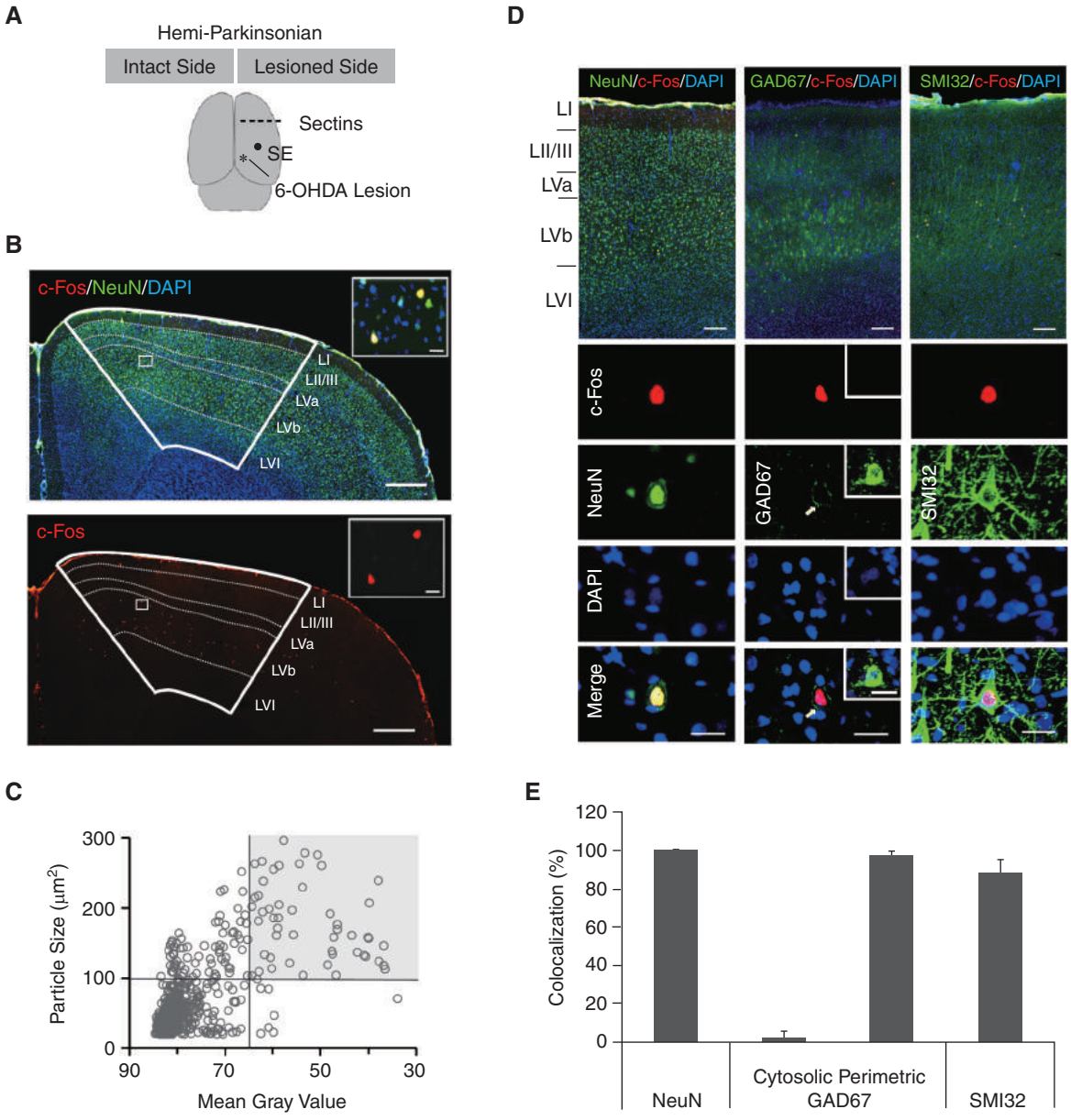

Fig 4. Characterization of giant FOS$^+$-particles in the motor cortex of hemi-Parkinsonian rats by Immunofluorescence staining. (A) Sites of operations in the brain. (B) A coronal section prepared from a hemi-Parkinsonian rat after receiving STN-HFS for 4 h and double immunostaining with the antibodies to c-Fos (red, bottom and top) and NeuN (green, top) and labeling with DAPI (blue, top). The motor cortex region is enclosed by white lines, and layers are separated by broken white lines. Scale bars: 500 μm. *top and bottom insets*: the regions enclosed by the white rectangles in the motor cortices at a higher magnification. Scale bar: 20 μm. (C) Scatter plot of the size (area, μm^2) and immunostaining intensity (mean gray level) of c-Fos$^+$-particles in the motor cortex on the lesioned side. (D) Coronal sections prepared from hemi-Parkinsonian rats after receiving STN-HFS for 4 h and immunofluorescence staining by the antibodies to c-Fos (red) and NeuN (Green) (left column images), by the antibodies to c-Fos (red) and GAD67 (green) (middle column images), and by the antibodies to c-Fos (red) and non-phosphorylated neurofilament heavy polypeptides (SMI32, green) (right column images). Sections are also labeled with DAPI (blue). Insets in the middle column images: a GABAergic neuron with GAD67-positive cytosol. Scale bars in top row images, in the images of the bottom 4 rows and in the insets are 200, 20 and 20 μm, respectively. (E) The fraction of giant FOS$^+$-particles exhibiting NeuN- and SMI32-positive immunoreactivity, fraction of giant FOS$^+$-particles surrounded by GAD67-positive punctas (labeled as perimetric), and fraction of giant FOS$^+$-particles with GAD67-positive cytosol (labeled as cytosolic). Images of (B) and (D) are from a representative experiment of a total of 3 independent experiments. Data in (C) are from 3 animals. Data in (E) are means ± S.D. from 3 animals.

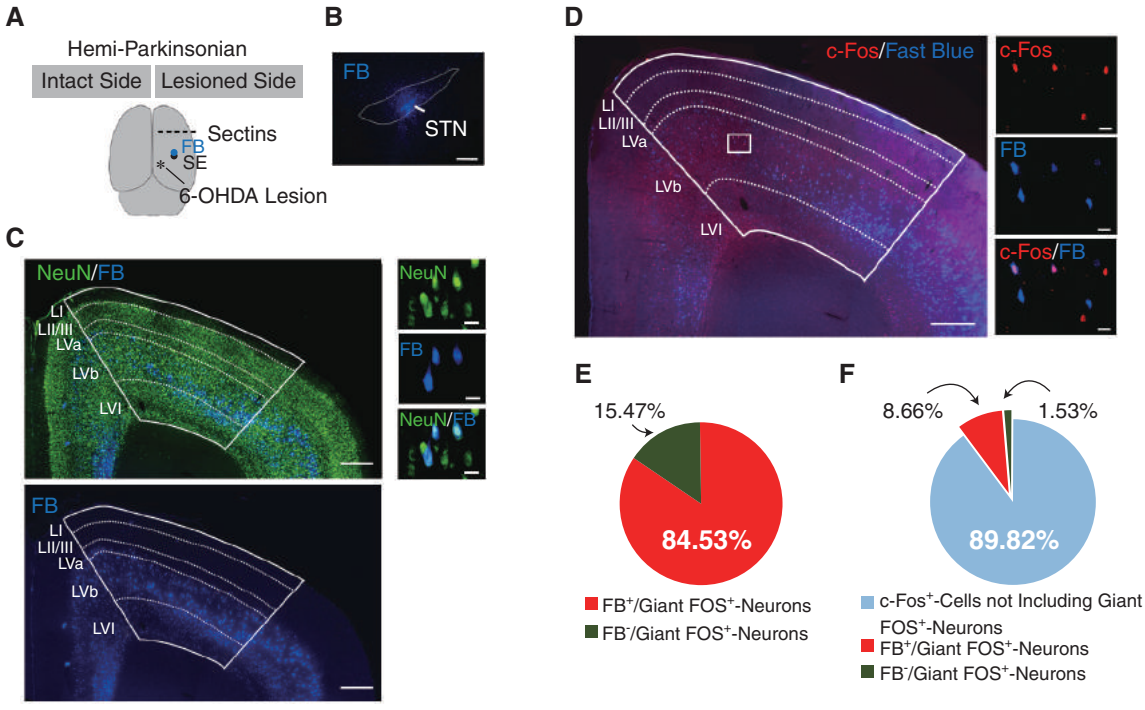

Fig 5. Back-labeling giant FOS$^+$-neurons in the motor cortex by Fast Blue applied to the STN. (A) Sits of operations in the brain. FB indicates the Fast Blue injection site. (B) Fast Blue (blue) in the STN (enclosed by white line). (C) Cells back-labeled by Fast Blue (blue) (left top and bottom images) in a coronal section prepared from a STN-HFS-treated hemi-Parkinsonian rat. Nearly all cells back-labeled with Fast Blue also exhibit NeuN immunoreactivity (right images). Scale bars in the left and right images are 500 and 20 μm, respectively. (D) Immunostaining the same section in (C) by anti-c-Fos antibody (red, left image) indicates that many giant FOS$^+$-neurons are back-labeled by Fast Blue (right images). The scale bars in the left and right images are 500 and 20 μm, respectively. (E) Pie chart showing the fractions of giant FOS$^+$-neurons which are or are not back-labeled by Fast Blue (red and green, respectively) of all the giant FOS$^+$-neurons in the motor cortex. A total of 179 Giant FOS$^+$-neurons are included in the calculation. (F) Pie chart showing the fractions of giant FOS$^+$-neurons that are or are not back-labeled Fast Blue (red and green, respectively) and the remaining c-Fos$^+$-cells (blue) in the motor cortex. 1834 c-Fos$^+$-cells are included in the calculation. Images in (C) and (D) are from a representative experiment of a total of 3 independent experiments with 3 animals. Data in (E) and (F) are from the data obtained from 3 animals.

Characterization of Giant FOS$^+$-Particles in the Motor Cortex by Immunofluorescence Staining

Brain sections prepared from the PD-S rats (Fig. 4A) were also subjected to immunofluorescence staining using an antibody to c-Fos (Fig. 4B, lower panel). In the motor cortex region of each section, 25.0 ± 3.3 (mean ± S.D., n = 3) giant FOS$^+$-particles, as c-Fos$^+$-particles with sizes >100 μm^2 and mean gray values <65 (Fig. 4C) and residing primarily in layer Vb (Fig. 4B, bottom panel) were also detected. Double fluorescence immunostaining was then used to characterize the giant FOS$^+$-particles. The results indicated that all giant FOS$^+$-particles exhibited the immunoreactivity of NeuN, a neuronal marker (Fig. 4B, top panel and inset; Figs. 4D & 4E, left column images). The giant FOS$^+$-particles were thus called as "giant FOS$^+$-neurons" henceforth. It was further found that the cytosol of the majority of the giant FOS$^+$-neurons, 87.8 ± 7.2% (n = 3), was positively stained by a SMI-32 antibody, which has been reported to recognize subcortical projecting layer V pyramidal neurons in the rat cortex (64, 68) (Figs. 4D & 4E, right column images). On the other hand, only 2.1 ± 3.5% (n = 3) of the giant FOS$^+$-neurons exhibited immunoreactivity of GAD67, a marker for GABAergic neurons, in the cytosol, and nearly all of them, 97.3 ± 2.1% (n = 3) were surrounded by GAD67-positive punctas (Figs. 4D & 4E, middle column images; a GAD67-positive puncta was indicated by arrow). This latter immunostaining pattern was different from that of the GABAergic neurons found in the same region, which exhibited GAD67 immunoreactivity in the cytosol (Fig. 4D, insets of the middle column images). Together, these results indicate that most giant FOS$^+$-neurons in the motor cortex are excitatory extracortical projection neurons.

Back-Labeling Giant FOS$^+$-Neurons in the Motor Cortex by Fast Blue Applied to Ipsilateral STN

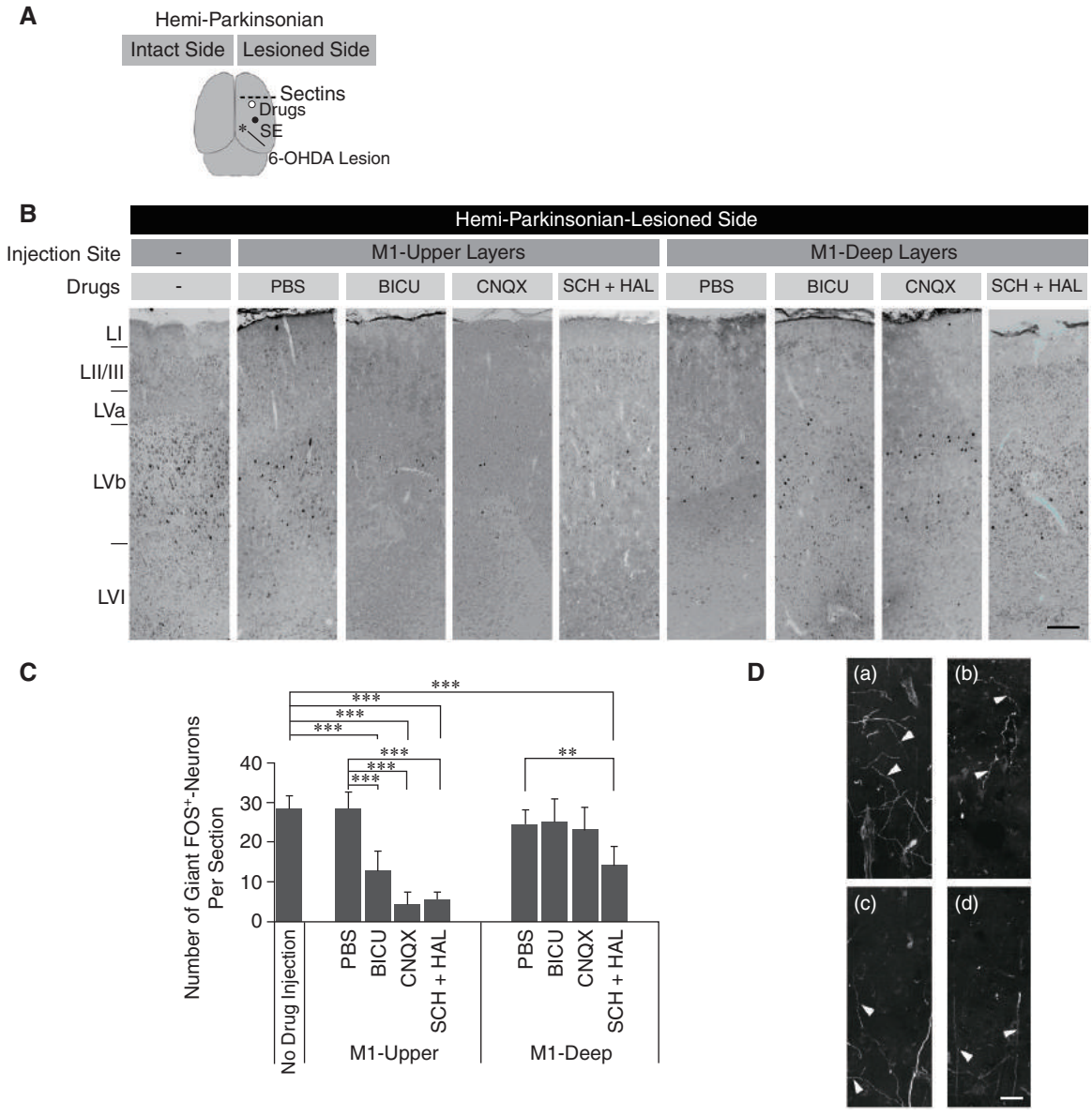

Fig 6. Effects of local application of CNQX, bicuculline and dopamine receptor antagonists SCH23390 and haloperidol on the induction of giant FOS$^+$-neurons in the motor cortex of STN-HFS-treated hemi-Parkinsonian rats. (A) Sites of operations in the brain. Drug application site is indicated by drugs. (B) c-Fos expression in the motor cortices ipsilateral to the stimulation and lesion sites of STN-HFS-treated hemi-Parkinsonian rats which have not or have received injection of PBS, CNQX (50 μM), bicuculline (50 μM, labeled as BICU) or a mixture containing SCH23390 (10 μM, labeled as SCH) and haloperidol (10 μM, labeled as HAL) into the upper or deep layers of M1. Scale bar: 200 μm. (C) Quantification of the numbers of giant FOS$^+$-neurons in the motor cortices of the hemi-Parkinsonian rats as described in (B). A total of 1,215 giant FOS$^+$-neurons are included in the analysis. Data are means ± S.D. from 6 sections prepared from 3 animals. $^{**}P < 0.01$ and $^{***}P < 0.001$. (D) TH-immunoreactive processes (arrowheads) in the layer II/III (a) and layer V (c) of the motor cortex in the intact side and in the layer II/III (b) and layer V (d) of the motor cortex in the lesioned side of a hemi-Parkinsonian rat. Scale bar: 25 μm.

Earlier studies have indicated that PT neurons send small-to-medium-sized axon collaterals to the STN (39, 62). To examine whether the giant FOS$^+$-neurons observed in this study might correspond to these PT neurons, we investigated if giant FOS$^+$-neurons could be back-labeled by Fast Blue applied to the STN in the lesioned side in the hemi-Parkinsonian rats (Fig. 5A). Two weeks after Fast Blue injection, hemi-Parkinsonian rats were subjected to STN-HFS and then immediately sacrificed. Fast Blue was detected in the STN of these animals (Fig. 5B). In the motor cortex of the brain sections prepared from these animals, many Fast Blue-back-labeled NeuN-positive cells were also observed (Fig. 5C),

and among these cells were the giant FOS^+-neurons (Fig. 5D). It was calculated that the majority of the giant FOS^+-neurons, 84.5 ± 1.2% (n = 3), exhibited the fluorescence of Fast Blue (Fig. 5E). In addition, it was calculated that the giant FOS^+-neurons accounted for 8.7 ± 1.7% (n = 3) of all c-Fos^+-cells found in the motor cortex (Fig. 5F). The results indicate that most giant FOS^+-neurons in the motor cortex send efferent projections to the STN. Together with the immunocytochemical characteristics as described in Fig. 4, the results suggest that most giant FOS^+-neurons found in the motor cortex in the lesioned side of STN-HFS-treated hemi-Parkinsonian rats are likely to correspond to the PT neurons, which send axonal collaterals to the STN as described earlier (39, 62, 68).

Effects of Local Drug Applications on the Number of Giant FOS^+-Neurons

To test if local synapses in the motor cortex contributed to the STN-HFS-induced intense c-Fos expression in the giant FOS^+-neurons, PBS, CNQX or bicuculline was applied to the deep or upper layers of the motor cortex, and these animals were then subjected to STN-HFS (Fig. 6A). CNQX and bicuculline are the antagonists of non-NMDA glutamate receptors and $GABA_A$ receptors, respectively, and the injection of these antagonists at 50 μM, or PBS, did not induce noticeable behavioral changes of the animals. It was found that injection of PBS into the upper or deep layers of the motor cortex did not affect the number of giant FOS^+-neurons found in the motor cortex (Figs. 6B & 6C, panels under "-" and "PBS"). Injection of CNQX or bicuculline to the upper layers, approximately in layers II/III, significantly reduced the number of giant FOS^+-neurons (Figs. 6B & 6C). On the other hand, injection of CNQX or bicuculline into the deeper layers, primarily in layer V, did not affect the number of giant FOS^+-neurons (Figs. 6B & 6C). These results indicate that non-NMDA glutamate receptors and $GABA_A$ receptors residing in the upper layers of the motor cortex are involved in inducing strong c-Fos expression in the giant FOS^+-neurons.

Hemi-Parkinsonian rats were also subjected to STN-HFS shortly after applying a mixture containing SCH-23390 and haloperidol, antagonists of D1 and D2 types of dopamine receptors, to the motor cortex in the hemi-Parkinsonian rats. The results indicated that the application of these antagonists to either the upper or deeper layers of the motor cortex reduced the number of giant FOS^+-neurons (Figs. 6B & 6C). However, applying these antagonists in the upper layer appeared to produce more pronounced inhibitory effects on the giant FOS^+-neurons than when the same antagonists were applied in the deeper layers (Figs. 6B & 6C). The results indicate that the activation of dopamine receptors in the motor cortex is also involved in the STN-HFS-induced strong c-Fos expression in the giant FOS^+-neurons.

To study if the motor cortex neurons in the lesioned side of the hemi-Parkinsonian rats still received dopaminergic input, the coronal brain sections containing the motor cortex prepared from the hemi-Parkinsonian rats were immunofluorescence stained using the TH antibody (Fig. 6D). In the motor cortex on the intact side, abundant fine TH-immunoreactive (ir) processes exhibiting numerous varicosities, similar to the catecholaminergic axons in the cerebral cortex as reported earlier (3), were observed (Fig. 6D, arrowheads in the left panels). TH-ir processes with similar morphologic characteristics were also observed in the motor cortex in the lesioned side (Fig. 6D, arrowheads in the right panels). However, much less TH-ir processes were observed in the lesioned side than in the intact side. The results indicate that in the hemi-Parkinsonian rats, the neurons in the motor cortex in the lesioned side still receive the input from small numbers of catecholaminergic axons, possibly including those of dopaminergic origin.

Discussion

Here, c-Fos expression was employed as an indicator to study how STN-HFS affects neuronal activities in the motor cortex of hemi-Parkinsonian rats. Our results indicated that STN-HFS rectified a bilateral imbalance between the motor cortices in the two hemispheres of the hemi-Parkinsonian rats with regard to the c-Fos^+-cell density. STN-HFS also induced strong c-Fos expression in a group of large cells, called the giant FOS^+-neurons here, residing primarily in layer Vb of the motor cortex in the lesioned side. By immunofluorescence staining, giant FOS^+-neurons was found to exhibit the biochemical characteristics of excitatory extracortical projecting neurons. Results from our back-labeling experiments further indicated that the majority of giant FOS^+-neurons sent efferent projections to the STN. These anatomical, biochemical and connectivity features are in accordance with that giant FOS^+-neurons correspond to the PT neurons, which send axonal collaterals to the STN (39, 49).

It is generally believed that when a neuron receives strong and sustained glutamatergic excitatory inputs along with GABA inhibitory modulation, c-Fos expression is rapidly turned on (12, 14). The intense c-Fos expression in the giant FOS^+-neurons as found in this work indicates that these neurons are strongly activated during STN-HFS. The STN-HFS stimulation could be conveyed from the STN to the motor cortex *via* the corticosubthalamic/corticospinal pathways

and other fibers running close to the STN in an antidromic direction; the STN stimulation could also be conveyed to the motor cortex *via* various efferent projection targets of the STN in an orthodromic direction (17, 27, 42, 43, 49). We observed here that the number of giant FOS^+-neurons was reduced by local application of CNQX and bicuculline in the motor cortex. This observation suggests that local circuit in the motor cortex, consisting of both glutamatergic and GABAergic synapses in the upper layers, may relay the STN-HFS stimulation *via* the abovementioned pathways to the giant FOS^+-neurons. In consistence, earlier electrophysiological studies have indicated that local circuit in the motor cortex is activated by HFS applied on the STN (17, 43).

We also observed that the number of giant FOS^+-neurons was reduced by applying dopamine receptor antagonists locally in the motor cortex, indicating that dopamine receptor activation plays an important role in the intense c-Fos expression in the giant FOS^+-neurons. Dopamine receptor activation may strengthen the synaptic inputs received by the giant FOS^+-neurons during STN-HFS by mechanisms including increases of intracellular [Ca^{2+}] and activation of various intracellular signaling pathways (1), thereby leading to enhanced c-Fos expression. However, why dopamine receptors in the motor cortex are activated during STN-HFS remains unknown. Dopamine plays important roles in modulating the neuronal activities and various functions of the motor cortex (31, 47, 67). Rat motor cortex receives dopaminergic input from two midbrain regions, the VTA and SNpc (32). Anatomical studies have indicated that STN sends projections to both SNpc and VTA (27). It has been reported that *via* the connections between STN and SNpc, STN-DBS leads to dopamine release from SNpc fibers in the striatum (7, 41). It has also been reported that electrically stimulating the VTA results in enhanced c-Fos expression of neurons in the motor cortex, possibly by elevation of extracellular dopamine (32). A possibility exists that HFS applied on the STN may induce dopamine release in the motor cortex from the residual fibers originating from the SNpc/VTA dopaminergic neurons, which have survived the 6-OHDA depletion operation (10, 66, and Fig. 6D in this study). Although the resultant increases in extracellular dopamine are expected to be low, it is likely that they could still activate dopamine receptors in the motor cortex because in the cortex of normal rats the background dopamine level is kept very low, at a concentration of ~1/20-1/50 of that in the striatum (23). By the same mechanism, the c-Fos expression in motor cortex neurons other than PT neurons may also be enhanced. As a result, when a hemi-Parkinsonian rat is subjected to STN-HFS, the bilateral imbalance between the densities of $c\text{-}Fos^+$-cells in the motor cortices in the two hemispheres is rectified. This observation appears to be in agreement with the study of Oueslani *et al*. (58) showing that the decrease of cytochrome oxidase subunit 1 mRNA level, as a marker of neuronal metabolic activity, in layer V of the motor cortex of 6-OHDA-lesioned rats was rectified by STN-HFS. Although both orthodromic and antidromic pathways mediating STN-HFS stimulation to the motor cortex exist in the brains of control and hemi-Parkinsonian rats (17, 43 and unpublished results of CF Chuang and YC Chang), STN-HFS-induced giant FOS^+-cells are detected in the PD, but seldom in the control animals. This difference suggests that a midbrain dopamine depletion operation performed on rats would result in alterations in the pathways mediating STN-HFS stimulation to the motor cortex in the resultant hemi-Parkinsonian rats.

The results obtained in this study indicate that STN-HFS activates neurons, including the PT neurons, in the motor cortex in the lesion side of hemi-Parkinsonian rats. On the basis of the observation that local application of dopamine receptor antagonists reduces the number of giant FOS^+-neurons, we speculate that STN-HFS may induce increases of extracellular dopamine in the motor cortex in hemi-Parkinsonian rats. In both human PD patients and hemi-Parkinsonian rats, reduced dopaminergic innervations in the motor cortex (21, 26) has been proposed to underlie, at least partly, the impaired motor functions and skill learning (31, 55). In patients with PD, dopamine has been found to modulate cortical functions (22, 38, 50), and STN-DBS could reduce and sometimes stop the patients' need for dopaminergic medications (53). STN-DBS induces dopamine release in the caudate and putamen of nonhuman primates and in the striatum of rodents (7, 20, 40, 51, 52). Whether STN-DBS also induces dopamine release in the motor cortex in human PD patients, and whether dopamine releases in the motor cortex contribute to the therapeutic effects of STN-DBS on alleviating the movement symptoms of PD need to be further investigated.

Acknowledgments

This work was supported by grants to YCC from the Ministry of Science and Technology (NSC 101-2627-E-007-001) and from the National Health Research Institute (NHRI-Ex105-10430N1) of Taiwan, Republic of China.

Conflict of Interests

The authors declare that they have no competing interests.

References

1. Beaulieu, J.M., Espinoza, S. and Gainetdinov, R.R. Dopamine receptors - IUPHAR Review 13. *Brit. J. Pharmacol.* 172: 1-23, 2015.
2. Benabid, A.L., Pollak, P., Louveau, A., Henry, S. and de Rougemont, J. Combined (thalamotomy and stimulation) stereotactic surgery of the VIM thalamic nucleus for bilateral Parkinson disease. *Appl. Neurophysiol.* 50: 344-346, 1987.
3. Benavides-Piccione, R. and DeFelipe, J. Distribution of neurons expressing tyrosine hydroxylase in the human cerebral cortex. *J. Anat.* 211: 212-222, 2007.
4. Blumenfeld, Z. and Bronte-Stewart, H. High frequency deep brain stimulation and neural rhythms in Parkinson's disease. *Neuropsychol. Rev.* 25: 384-397, 2015.
5. Boix, J., Padel, T. and Paul, G. A partial lesion model of Parkinson's disease in mice--characterization of a 6-OHDA-induced medial forebrain bundle lesion. *Behav. Brain Res.* 284: 196-206, 2015.
6. Boraud, T., Bezard, E., Bioulac, B. and Gross, C. High frequency stimulation of the internal Globus Pallidus (GPi) simultaneously improves parkinsonian symptoms and reduces the firing frequency of GPi neurons in the MPTP-treated monkey. *Neurosci. Lett.* 215: 17-20, 1996.
7. Bruet, N., Windels, F., Bertrand, A., Feuerstein, C., Poupard, A. and Savasta, M. High frequency stimulation of the subthalamic nucleus increases the extracellular contents of striatal dopamine in normal and partially dopaminergic denervated rats. *J. Neuropathol. Exp. Neurol.* 60: 15-24, 2001.
8. Carron, R., Chaillet, A., Filipchuk, A., Pasillas-Lepine, W. and Hammond, C. Closing the loop of deep brain stimulation. *Front. Syst. Neurosci.* 7: 112, 2013.
9. Chaudhuri, A. Neural activity mapping with inducible transcription factors. *Neuroreport* 8: v-ix, 1997.
10. Chen, L., Liu, Z., Tian, Z., Wang, Y. and Li, S. Prevention of neurotoxin damage of 6-OHDA to dopaminergic nigral neuron by subthalamic nucleus lesions. *Stereotact. Funct. Neurosurg.* 75: 66-75, 2000.
11. Chiken, S. and Nambu, A. Mechanism of deep brain stimulation: inhibition, excitation, or disruption? *Neuroscientist* 22: 313-322, 2016.
12. Cohen, S. and Greenberg, M.E. Communication between the synapse and the nucleus in neuronal development, plasticity, and disease. *Annu. Rev. Cell Dev. Biol.* 24: 183-209, 2008.
13. Contarino, M.F., Bour, L.J., Verhagen, R., Lourens, M.A., de Bie, R.M., van den Munckhof, P. and Schuurman, P.R. Directional steering: A novel approach to deep brain stimulation. *Neurology* 83: 1163-1169, 2014.
14. Cruz, F.C., Koya, E., Guez-Barber, D.H., Bossert, J.M., Lupica, C.R., Shaham, Y. and Hope, B.T. New technologies for examining the role of neuronal ensembles in drug addiction and fear. *Nat. Rev. Neurosci.* 14: 743-754, 2013.
15. Delaville, C., Cruz, A.V., McCoy, A.J., Brazhnik, E., Avila, I., Novikov, N. and Walters, J.R. Oscillatory activity in basal ganglia and motor cortex in an awake behaving rodent model of Parkinson's disease. *Basal Ganglia* 3: 221-227, 2014.
16. DeLong, M.R. and Benabid, A.L. Discovery of high-frequency deep brain stimulation for treatment of Parkinson disease: 2014 Lasker Award. *JAMA* 312: 1093-1094, 2014.
17. Devergnas, A. and Wichmann, T. Cortical potentials evoked by deep brain stimulation in the subthalamic area. *Front. Syst. Neurosci.* 5: 30, 2011.
18. Elahi, B., Elahi, B. and Chen, R. Effect of transcranial magnetic stimulation on Parkinson motor function--systematic review of controlled clinical trials. *Mov. Disord.* 24: 357-363, 2009.
19. Gage, G.J., Kipke, D.R. and Shain, W. Whole animal perfusion fixation for rodents. *J. Vis. Exp.* 2012.
20. Gale, J.T., Lee, K.H., Amirnovin, R., Roberts, D.W., Williams, Z.M., Blaha, C.D. and Eskandar, E.N. Electrical stimulation-evoked dopamine release in the primate striatum. *Stereotact. Funct. Neurosurg.* 91: 355-363, 2013.
21. Gaspar, P., Duyckaerts, C., Alvarez, C., Javoy-Agid, F. and Berger, B. Alterations of dopaminergic and noradrenergic innervations in motor cortex in Parkinson's disease. *Ann. Neurol.* 30: 365-374, 1991.
22. George, J.S., Strunk, J., Mak-McCully, R., Houser, M., Poizner, H. and Aron, A.R. Dopaminergic therapy in Parkinson's disease decreases cortical beta band coherence in the resting state and increases cortical beta band power during executive control. *Neuroimage Clin.* 3: 261-270, 2013.
23. Godefroy, F., Bassant, M.H., Weil-Fugazza, J. and Lamour, Y. Age-related changes in dopaminergic and serotonergic indices in the rat forebrain. *Neurobiol. Aging.* 10: 187-190, 1989.
24. Gradinaru, V., Mogri, M., Thompson, K.R., Henderson, J.M. and Deisseroth, K. Optical deconstruction of parkinsonian neural circuitry. *Science* 324: 354-359, 2009.
25. Gutierrez, J.C., Seijo, F.J., Alvarez Vega, M.A., Fernandez Gonzalez, F., Lozano Aragoneses, B. and Blazquez, M. Therapeutic extradural cortical stimulation for Parkinson's disease: report of six cases and review of the literature. *Clin. Neurol. Neurosurg.* 111: 703-707, 2009.
26. Halje, P., Tamte, M., Richter, U., Mohammed, M., Cenci, M.A. and Petersson, P. Levodopa-induced dyskinesia is strongly associated with resonant cortical oscillations. *J. Neurosci.* 32: 16541-16551, 2012.
27. Hamani, C., Saint-Cyr, J.A., Fraser, J., Kaplitt, M. and Lozano, A.M. The subthalamic nucleus in the context of movement disorders. *Brain* 127: 4-20, 2004.
28. Herman, J.P., Rouge-Pont, F., Le Moal, M. and Abrous, D.N. Mechanisms of amphetamine-induced rotation in rats with unilateral intrastriatal grafts of embryonic dopaminergic neurons: a pharmacological and biochemical analysis. *Neuroscience* 53: 1083-1095, 1993.
29. Herrington, T.M., Cheng, J.J. and Eskandar, E.N. Mechanisms of deep brain stimulation. *J. Neurophysiol.* 115: 19-38, 2016.
30. Hickey, P. and Stacy, M. Deep brain stimulation: a paradigm shifting approach to treat Parkinson's disease. *Front. Neurosci.* 10: 173, 2016.
31. Hosp, J.A. and Luft, A.R. Dopaminergic meso-cortical projections to m1: role in motor learning and motor cortex plasticity. *Front. Neurol.* 4: 145, 2013.
32. Hosp, J.A., Pekanovic, A., Rioult-Pedotti, M.S. and Luft, A.R. Dopaminergic projections from midbrain to primary motor cortex mediate motor skill learning. *J. Neurosci.* 31: 2481-2487, 2011.
33. Hsu, C.I., Ho, T.S., Liou, Y.R. and Chang, Y.C. Morphological changes and synaptogenesis of corticothalamic neurons in the somatosensory cortex of rat during perinatal development. *Cereb. Cortex* 21: 884-895, 2011.
34. Iancu, R., Mohapel, P., Brundin, P. and Paul, G. Behavioral characterization of a unilateral 6-OHDA-lesion model of Parkinson's disease in mice. *Behav. Brain Res.* 162: 1-10, 2005.
35. Jankovic, J. and Aguilar, L.G. Current approaches to the treatment of Parkinson's disease. *Neuropsychiatr. Dis. Treat.* 4: 743-757, 2008.
36. Jenkinson, N. and Brown, P. New insights into the relationship between dopamine, beta oscillations and motor function. *Trends Neurosci.* 34: 611-618, 2011.
37. Katzenschlager, R. and Lees, A.J. Treatment of Parkinson's disease: levodopa as the first choice. *J. Neurol.* 249 (Suppl 2): ii19-ii24, 2002.
38. Kawashima, S., Ueki, Y., Mima, T., Fukuyama, H., Ojika, K. and Matsukawa, N. Differences in dopaminergic modulation to motor cortical plasticity between Parkinson's disease and multiple system atrophy. *PLoS One* 8: e62515, 2013.

39. Kita, T. and Kita, H. The subthalamic nucleus is one of multiple innervation sites for long-range corticofugal axons: a single-axon tracing study in the rat. *J. Neurosci.* 32: 5990-5999, 2012.
40. Lee, K.H., Blaha, C.D., Harris, B.T., Cooper, S., Hitti, F.L., Leiter, J.C., Roberts, D.W. and Kim, U. Dopamine efflux in the rat striatum evoked by electrical stimulation of the subthalamic nucleus: potential mechanism of action in Parkinson's disease. *Eur. J. Neurosci.* 23: 1005-1014, 2006.
41. Lester, D.B., Rogers, T.D. and Blaha, C.D. Neuronal pathways involved in deep brain stimulation of the subthalamic nucleus for treatment of Parkinson's disease. *Conf. Proc. IEEE Eng. Med. Biol. Soc.* 2009: 3302-3305, 2009.
42. Li, Q., Ke, Y., Chan, D.C., Qian, Z.M., Yung, K.K., Ko, H., Arbuthnott, G.W. and Yung, W.H. Therapeutic deep brain stimulation in Parkinsonian rats directly influences motor cortex. *Neuron* 76: 1030-1041, 2012.
43. Li, S., Arbuthnott, G.W., Jutras, M.J., Goldberg, J.A. and Jaeger, D. Resonant antidromic cortical circuit activation as a consequence of high-frequency subthalamic deep-brain stimulation. *J. Neurophysiol.* 98: 3525-3537, 2007.
44. Lin, Y.P., Yeh, C.Y., Huang, P.Y., Wang, Z.Y., Cheng, H.H., Li, Y.T., Chuang, C.F., Huang, P.C., Tang, K.T., Ma, H.P., Chang, Y.C., Yeh, S.R. and Chen, H. A battery-less, implantable neuroelectronic interface for studying the mechanisms of deep brain stimulation in rat models. *I EEE Trans. Biomed. Circuits Syst.* 10: 98-112, 2016.
45. Lindemann, C., Krauss, J.K. and Schwabe, K. Deep brain stimulation of the subthalamic nucleus in the 6-hydroxydopamine rat model of Parkinson's disease: effects on sensorimotor gating. *Behav. Brain Res.* 230: 243-250, 2012.
46. Lindenbach, D. and Bishop, C. Critical involvement of the motor cortex in the pathophysiology and treatment of Parkinson's disease. *Neurosci. Biobehav. Rev.* 37: 2737-2750, 2013.
47. Luft, A.R. and Schwarz, S. Dopaminergic signals in primary motor cortex. *Int. J. Dev. Neurosci.* 27: 415-421, 2009.
48. Maesawa, S., Kaneoke, Y., Kajita, Y., Usui, N., Misawa, N., Nakayama, A. and Yoshida, J. Long-term stimulation of the subthalamic nucleus in hemiparkinsonian rats: neuroprotection of dopaminergic neurons. *J. Neurosurg.* 100: 679-687, 2004.
49. Mathai, A. and Smith, Y. The corticostriatal and corticosubthalamic pathways: two entries, one target. So what? *Front. Syst. Neurosci.* 5: 64, 2011.
50. Mattay, V.S., Tessitore, A., Callicott, J.H., Bertolino, A., Goldberg, T.E., Chase, T.N., Hyde, T.M. and Weinberger, D.R. Dopaminergic modulation of cortical function in patients with Parkinson's disease. *Ann. Neurol.* 51: 156-164, 2002.
51. Meissner, W., Harnack, D., Reese, R., Paul, G., Reum, T., Ansorge, M., Kusserow, H., Winter, C., Morgenstern, R. and Kupsch, A. High-frequency stimulation of the subthalamic nucleus enhances striatal dopamine release and metabolism in rats. *J. Neurochem.* 85: 601-609, 2003.
52. Min, H.K., Ross, E.K., Jo, H.J., Cho, S., Settell, M.L., Jeong, J.H., Duffy, P.S., Chang, S.Y., Bennet, K.E., Blaha, C.D. and Lee, K.H. Dopamine release in the nonhuman primate caudate and putamen depends upon site of stimulation in the subthalamic nucleus. *J. Neurosci.* 36: 6022-6029, 2016.
53. Moro, E., Scerrati, M., Romito, L.M., Roselli, R., Tonali, P. and Albanese, A. Chronic subthalamic nucleus stimulation reduces medication requirements in Parkinson's disease. *Neurology* 53: 85-90, 1999.
54. Murrow, R.W. Penfield's prediction: a mechanism for deep brain stimulation. *Front. Neurol.* 5: 213, 2014.
55. O'Donnell, P. Dopamine gating of forebrain neural ensembles. *Eur. J. Neurosci.* 17: 429-435, 2003.
56. Odekerken, V.J., Boel, J.A., Schmand, B.A., de Haan, R.J., Figee, M., van den Munckhof, P., Schuurman, P.R., de Bie, R.M. and NSTAPS study group. GPi *vs* STN deep brain stimulation for Parkinson disease: Three-year follow-up. *Neurology* 86: 755-761, 2016.
57. Oertel, W. and Schulz, J.B. Current and experimental treatments of Parkinson disease: A guide for neuroscientists. *J. Neurochem.* 139 (Suppl 1): 325-337, 2016.
58. Oueslati, A., Sgambato-Faure, V., Melon, C., Kachidian, P., Gubellini, P., Amri, M., Kerkerian-Le Goff, L. and Salin, P. High-frequency stimulation of the subthalamic nucleus potentiates L-DOPA-induced neurochemical changes in the striatum in a rat model of Parkinson's disease. *J. Neurosci.* 27: 2377-2386, 2007.
59. Pahwa, R., Wilkinson, S., Smith, D., Lyons, K., Miyawaki, E. and Koller, W.C. High-frequency stimulation of the globus pallidus for the treatment of Parkinson's disease. *Neurology* 49: 249-253, 1997.
60. Perese, D.A., Ulman, J., Viola, J., Ewing, S.E. and Bankiewicz, K.S. A 6-hydroxydopamine-induced selective parkinsonian rat model. *Brain Res.* 494: 285-293, 1989.
61. Rosin, B., Slovik, M., Mitelman, R., Rivlin-Etzion, M., Haber, S.N., Israel, Z., Vaadia, E. and Bergman, H. Closed-loop deep brain stimulation is superior in ameliorating parkinsonism. *Neuron* 72: 370-384, 2011.
62. Shepherd, G.M. Corticostriatal connectivity and its role in disease. *Nat. Rev. Neurosci.* 14: 278-291, 2013.
63. Siegfried, J. and Shulman, J. Deep brain stimulation. *Pacing Clin. Electrophysiol.* 10: 271-272, 1987.
64. Staal, J.A., Alexander, S.R., Liu, Y., Dickson, T.D. and Vickers, J.C. Characterization of cortical neuronal and glial alterations during culture of organotypic whole brain slices from neonatal and mature mice. *PLoS One* 6: e22040, 2011.
65. Tass, P.A., Qin, L., Hauptmann, C., Dovero, S., Bezard, E., Boraud, T. and Meissner, W.G. Coordinated reset has sustained aftereffects in Parkinsonian monkeys. *Ann. Neurol.* 72: 816-820, 2012.
66. Torres, E.M., Lane, E.L., Heuer, A., Smith, G.A., Murphy, E. and Dunnett, S.B. Increased efficacy of the 6-hydroxydopamine lesion of the median forebrain bundle in small rats, by modification of the stereotaxic coordinates. *J. Neurosci. Methods* 200: 29-35, 2011.
67. Vitrac, C., Peron, S., Frappe, I., Fernagut, P.O., Jaber, M., Gaillard, A. and Benoit-Marand, M. Dopamine control of pyramidal neuron activity in the primary motor cortex *via* D2 receptors. *Front. Neural Circuits* 8: 13, 2014.
68. Voelker, C.C., Garin, N., Taylor, J.S., Gahwiler, B.H., Hornung, J.P. and Molnar, Z. Selective neurofilament (SMI-32, FNP-7 and N200) expression in subpopulations of layer V pyramidal neurons *in vivo* and *in vitro*. *Cereb. Cortex* 14: 1276-1286, 2004.